HEFAT2014
10th International Conference on Heat Transfer, Fluid Mechanics and Thermodynamics
14 – 16 July 2014
Orlando, Florida

A LOCALLY-INTEGRATED MESHLESS (LIM) METHOD APPLIED TO ADVECTION-DIFFUSION PROBLEMS

Divo E.A[1,*] and Kassab A.J.[2]
[1]Department of Mechanical Engineering,
Embry-Riddle Aeronautical University,
Daytona Beach, FL 32114, USA
[*]E-mail: divoe@erau.edu
[2]Department of Mechanical and Aerospace Engineering,
University of Central Florida,
Orlando, FL 32816, USA

ABSTRACT

A new numerical solution scheme coined as the LIM (Locally-Integrated Meshless) method is formulated in this paper. As a Meshless formulation the LIM Method relies uniquely on a scattered non-ordered data point distribution within the domain of interest and does not require connectivity or polygonalization. In the LIM method formulation the field variable is approximated within localized overlapping regions containing a predetermined number of data points, as a linear combination of predefined expansion functions. These expansion functions are chosen in this study to be the well-known Hardy Multiquadrics Radial-basis functions (RBF) with center at the data points within each localized region. A weighted-residual integration is applied on each region to minimize the difference between the approximated field and the exact one. In order to circumvent the integration of an unavailable exact field, the residual integral is decomposed into a collocation integral (weights are set to Dirac delta functions) and a fully-weighted integral, resulting in a formulation where the coefficients of the expansion can be expressed directly in terms of the values of the field variable at the data points. This approach allows mitigating the issues that arise when performing direct collocation where the resulting derivative fields are sensitive and inaccurate due to the 'anchoring' of the expansion to the data points. In contrast, the LIM yields derivative fields that are smooth and accurate as they are rendered from a 'non-anchored' expansion while providing the ability to express the expansion coefficients, and thus the derivative fields, directly in terms of the scattered data within each local region. This combination of features is critical for the implementation of the LIM method as a robust, stable, and accurate solution scheme of governing differential equations.

INTRODUCTION

In recent history, the area of physics-based engineering simulation has seen rapid increases in both computer workstation performance as well as common engineering model complexity, both driven largely in part by advances in memory density and availability of clusters and multi-core processors.

While the increase in computation time due to model complexity has been largely offset by the increased performance of modern workstations, the increase in model setup time due to model complexity has continued to rise. As such, the major time requirement for solving an engineering model has transitioned from computation time to problem setup time. This is due to the fact that developing the required mesh for complex geometries can be an extremely complicated and time consuming task, and consequently, new solution techniques that can reduce the required amount of human interaction are desirable.

While the finite element method (FEM) and the boundary element method (BEM) have been developed to a mature stage such that they are now utilized routinely to model complex multi-physics problems, they require significant effort in formulation, mesh generation, and data management.

NOMENCLATURE

$\phi_j(x), \psi_j(x)$	[-]	Multiquadrics Radial-basis functions (RBF)
$r_j(x)$	[m]	Euclidean distance between points x and x_j
c	[m]	RBF shape parameter
α_j, β_j	[-]	RBF expansion coefficients
Ω	[m^3]	Domain of interest
R_Ω	[-]	Domain residual
$w(x)$	[-]	Weight function
$\{L\}$	[-]	Derivative interpolation vector
$T(x)$	[K]	Temperature field
$\vec{V}(x)$	[m/s]	Velocity Field
ρ	[kg/m^3]	Density
c_p	[J/kgK]	Specific heat capacity
k	[W/mK]	Thermal conductivity

Meshless methods are a relative newcomer to the field of computational methods. The term "Meshless Methods" refers to the class of numerical techniques that rely on either global or localized interpolation on non-ordered spatial point distributions. As such, there has been much interest in the development of these techniques as they have the hope of reducing the effort devoted to model preparation [1]-[7]. The approach finds its origin in classical spectral or pseudo-spectral methods [8]-[12] that are based on global orthogonal functions such as Legendre or Chebyshev polynomials requiring a regular nodal point distribution. In contrast, Meshless methods use a nodal or point distribution that is not required to be uniform or regular due to the fact that most such techniques rely on global radial-basis functions (RBF) [13]-[23]. RBF have proved quite successful in their application to an earlier mesh-reduction method, namely the dual reciprocity boundary element method (DRBEM) [24], [25]. However, global RBF-based Meshless methods have some drawbacks including poor conditioning of the ensuing algebraic set of equations which can be addressed to some extent by domain decomposition and appropriate pre-conditioning [20]. Moreover, care must be taken in the evaluation of derivatives in global RBF-based Meshless methods. Although, very promising, these techniques can also be computationally intensive. Recently, localized collocation Meshless methods [26]-[28] have been proposed to address many of the issues posed by global RBF Meshless methods.

For more than a decade the co-authors have been involved in numerical modeling of heat transfer, fluid flow, and solid mechanics problems using Boundary Element Methods (BEM), its derivative, Dual Reciprocity BEM, and other mesh reduction techniques, see [24], [25], [29]-[32]. In a series of recent publications [33]-[51], the co-authors have developed a Localized Collocation Meshless (LCM) Method based on Radial-Basis Function (RBF) interpolation for modeling of coupled viscous fluid flow, heat transfer problems, and fluid-structure interaction problems. The LCMM features Hardy Multiquadrics RBF augmented by polynomial expansions over a local topology of points for the sought-after unknowns with an efficient formulation for computing the interpolations in terms of vector products. This approach is applicable to explicit or implicit time marching schemes as well as steady-state iterative methods. The LCMM technique lends itself very well to parallel computations. In recent publications [41]-[43], [45]-[51], the LCMM is shown to be computationally more efficient than a comparative Finite Volume Method (FVM) code whilst affording the distinct advantage of solving the partial differential conservation field equations of fluid flow and heat transfer on a non-ordered set of points. The method has been extensively verified against benchmarks and validated finite volume codes for several cases.

COLLOCATED VS. WEIGHTED RBF EXPANSION

Assume a general function $f(x)$ may be approximated as $f_a(x)$ within a domain Ω by expanding it in terms of a linear combination of N predefined expansion functions $\phi_j(x)$, as:

$$f_a(x) = \sum_{j=1}^{N} \alpha_j \phi_j(x) \qquad (1)$$

The choice of functions $\phi_j(x)$ dictates the nature of the expansion. For instance, the expansion functions $\phi_j(x)$ may be selected from the family of Radial-Basis functions (RBF). Such functions consist of algebraic expressions uniquely defined in terms of the Euclidean distance $r_j(x)$ from a general field point x to an expansion point $x_j \therefore j = 1 \ldots N$ within the domain Ω. One example of these RBF is the well-established inverse Multiquadrics RBF, [17], defined as:

$$\phi_j(x) = \left[\left(\frac{r_j(x)}{c} \right)^2 + 1 \right]^{-\frac{1}{2}} \qquad (2)$$

The behavior of this function has been largely studied in the literature, [14], [21], [23]. However, the so-called shape parameter c single-handedly dictates the behavior of the expansion and, more importantly, its derivatives. Specifically, the larger the shape parameter c the flatter the functions $\phi_j(x)$ become and, therefore, the smoother the derivative field. However, this shape parameter cannot be increased boundless because as the expansion functions become 'flatter' the resulting algebraic system to determine the expansion coefficients α_j becomes ill-conditioned, see [41]-[43]. A simple search process to determine the optimal value of this shape parameter has been shown to be effective.

In order to minimize the difference between the function $f(x)$ and its approximation $f_a(x)$, a residual R_Ω may be defined such that the integrated weighted difference between these functions vanishes, hence:

$$R_\Omega = \int_\Omega \left[f_a(x) - f(x) \right] w(x) d\Omega = 0 \qquad (3)$$

The choice of weighting function $w(x)$ in the residual R_Ω definition dictates the nature of the interpolation of the function $f(x)$. For instance, if the weighting function $w(x)$ is chosen to be a set of Dirac Delta functions $\delta(x, x_i)$ centered at the same expansion points $x_i \therefore i = 1 \ldots N$ where the RBF expansion functions $\phi_j(x)$ are referenced. This choice of weighting functions leads to:

$$\int_\Omega \left[\sum_{j=1}^{N} \alpha_j \phi_j(x) - f(x) \right] \delta(x, x_i) d\Omega = 0 \qquad (4)$$

This expression can be rearranged as:

$$\sum_{j=1}^{N} \alpha_j \int_\Omega \phi_j(x)\delta(x, x_i)d\Omega = \int_\Omega f(x)\delta(x, x_i)d\Omega \quad (5)$$

Taking advantage of the 'Sifting' property of the Dirac Delta function results in:

$$\sum_{j=1}^{N} \alpha_j \phi_j(x_i) = f(x_i) \quad (6)$$

The expression in Eqn. (6) represents a standard 'collocation' of the function $f(x)$ at the scattered locations $x_i \therefore i = 1 \ldots N$ within the domain Ω. This results in a simple expression for the expansion coefficients α_j, such that:

$$\{\alpha\} = [\phi]^{-1}\{f\} \quad (7)$$

The main advantage of following the 'collocation' approach is that the exact distribution of the function to be expanded $f(x)$ needs not be known but instead simple scattered information $\{f\}$ is sufficient to achieve the expansion. In addition, the resulting expansion $f_a(x)$ is exact at the scattered locations $x_i \therefore i = 1 \ldots N$. The issue with this is that 'anchoring' the expansion at these scattered locations results in inaccurate derivative fields $\partial f_a(x)$.

On the other hand if a 'weighted' rather than a 'collocated' approach is followed, the resulting expression for the expansion coefficients α_j is:

$$\sum_{j=1}^{N} \alpha_j \int_\Omega \phi_j(x)w(x, x_i)d\Omega = \int_\Omega f(x)w(x, x_i)d\Omega \quad (8)$$

Or in matrix-vector form:

$$\{\alpha\} = [\phi_w]^{-1}\{f_w\} \quad (9)$$

Construction of the coefficient vector $\{f_w\}$ on the right-hand side of Eqn. (9) requires the exact distribution of the function $f(x)$ to be known, therefore, this expansion is not possible if only scattered information about this function $\{f\}$ is known. However, since the resulting expansion $f_a(x)$ is not 'anchored' at the expansion points, its derivative field is smoother and more accurate.

Example of Collocated and Weighted RBF Expansion

An example drawing a comparison between an RBF collocation expansion and an RBF weighted expansion over a domain of interest Ω as a 1×1 square is presented. The function to be tested is:

$$f(x, y) = \sin(\pi y)\cosh\left(\frac{1-x}{2}\right) / \cosh\left(\frac{1}{2}\right) \quad (10)$$

A total of $N = 25$ points to serve as data centers for the Multiquadrics RBF in Eqn. (2) are equally distributed in this domain. The point distribution and the test function contour plot are shown in Figure 1.

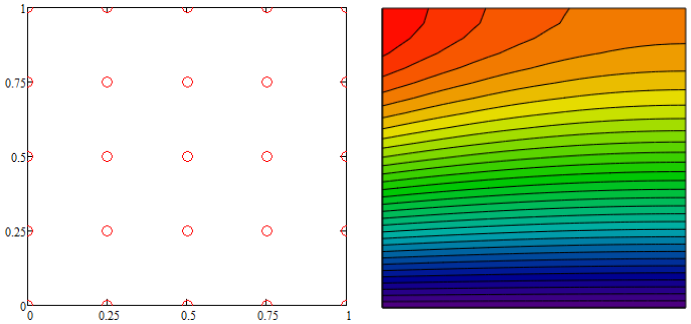

Figure 1 Geometry and point distribution of RBF test case.

The collocation is performed using the Multiquadrics RBF in Eqn. (2) with a shape parameter $c = 6$ which yields a condition number for the collocation matrix of 10^{16}. The weighted expansion is performed using a weight function:

$$w(x, x_i) = \frac{1}{2\pi}\ln[r_i(x)] \quad (11)$$

The choice of this weight function will be clarified in the next section. Notice that the weight function introduces a singularity when evaluated at the data center $r_i(x) = 0$, however, this singularity is weak and eliminated when integrating over the domain. The same RBF with the same shape parameter are employed for the weighted expansion yielding a condition number for the expansion matrix of 10^{15}.

Plots of the *x*-derivative, *y*-derivative, and *Laplacian* of the test function are shown in Figure 2, Figure 3, and Figure 4 revealing very high qualitative accuracy. However, the quantitative results of these values at the domain center $(0.5, 0.5)$ as well as the RMS errors throughout the domain shown in

Table **1** reveal that the weighted approach performs significantly better than the collocated approach**.**

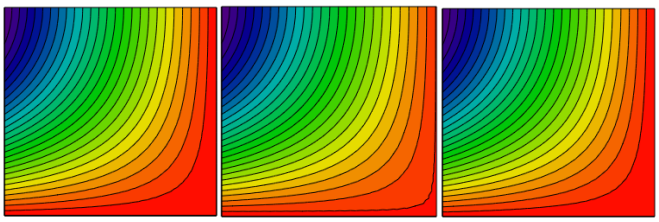

Figure 2 Exact, collocated, and weighted $\partial f / \partial x$

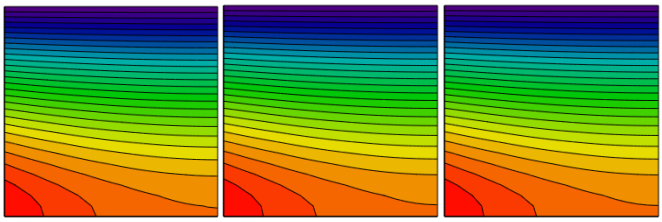

Figure 3 Exact, collocated, and weighted $\partial f / \partial y$

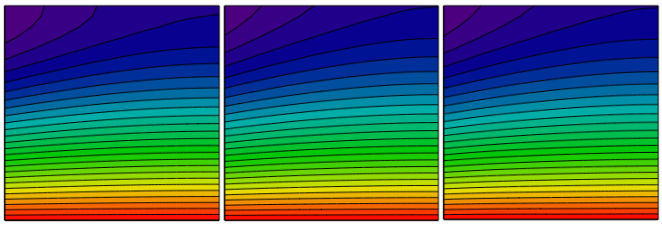

Figure 4 Exact, collocated, and weighted $\nabla^2 f$

Table 1 Exact, collocated, and weighted values and norms

	Exact	**Collocated**		**Weighted**	
		(0.5,0.5)	*RMS*	*(0.5,0.5)*	*RMS*
$\partial f / \partial x$	-0.079	-0.085	0.125	-0.079	0.005
$\partial f / \partial y$	1.016	1.018	0.073	1.015	0.016
$\nabla^2 f$	-1.434	-1.450	0.488	-1.433	0.291

HYBRID RBF EXPANSION

In order to mitigate the issues that arise when performing direct collocation where the resulting derivative field is inaccurate due to the 'anchoring' of the expansion, a hybrid approach is proposed so that the advantage offered by collocation of allowing expansion of a scattered field is preserved, while the advantages offered by the a weighted expansion are also enjoyed, in particular, the resulting derivative field is smooth and accurate as it is rendered from a 'non-anchored' expansion. This combination of features is critical for the implementation of RBF expansions in the solution of governing differential equations for a robust and accurate Meshless Method, in particular, a Localized Meshless Method.

Assume again a general function $f(x)$ available only in discrete form $\{f\}$ at a set of scattered points $x_i \therefore i = 1 \ldots N$ within a domain Ω. This function can be approximated as $f_c(x)$ by an RBF expansion of the form:

$$f_c(x) = \sum_{j=1}^{N} \alpha_j \phi_j(x) \tag{12}$$

In addition, assume that the function can also be approximated as $f_w(x)$ by another RBF expansion of the form:

$$f_w(x) = \sum_{j=1}^{N} \beta_j \psi_j(x) \tag{13}$$

In order to minimize the difference between the function $f(x)$ and its approximations $f_c(x)$ and $f_w(x)$, a combined residual, R_Ω, may be defined such that the integrated weighted differences between these functions vanishes as:

$$\begin{aligned} R_\Omega &= \int_\Omega \left[f_c(x) - f(x) \right] w_c(x) d\Omega \\ &+ \int_\Omega \left[f_w(x) - f(x) \right] w(x) d\Omega = 0 \end{aligned} \tag{14}$$

Now, let the two weighting functions $w_c(x)$ and $w(x)$ relate to each other as:

$$w_c(x) = \nabla^2 w(x) - w(x) \tag{15}$$

This expression is rather arbitrary but it allows relating the two weighting functions to each other as well as the ultimate purpose of explicitly separating the residual expression to form a weighted approximation of the function only in terms of its scattered information.

Introducing the definition in Eqn. (15) into Eqn. (14) results in:

$$\begin{aligned} &\int_\Omega \left[f_c(x) - f(x) \right] \nabla^2 w(x) d\Omega \\ &+ \int_\Omega \left[f_w(x) - f_c(x) \right] w(x) d\Omega = 0 \end{aligned} \tag{16}$$

Furthermore, the first integral on the left-hand side of Eqn. (16) can be defined as a residual R_c and allowed to vanish while the second integral on the left-hand side of Eqn. (16) can be defined as a residual R_w that vanishes as well. That is:

$$R_c = \int_\Omega \left[f_c(x) - f(x) \right] \nabla^2 w(x) d\Omega = 0 \tag{17}$$

And, therefore:

$$R_w = \int_\Omega \left[f_w(x) - f_c(x) \right] w(x) d\Omega = 0 \tag{18}$$

The next step consists in selecting the weighting function $w(x)$. An obvious choice will be to allow it to obey the following:

$$\nabla^2 w(x) = \delta(x, x_i) \tag{19}$$

So that the expansion resulting from the residual R_c in Eqn. (17) is a direct collocation, and, therefore:

$$\{\alpha\} = [\phi]^{-1}\{f\} \tag{20}$$

Furthermore, the weighting function $w(x)$ can be solved for directly from Eqn. (19), resulting in the well-known free-space solution:

$$\begin{aligned} w(x, x_i) &= \frac{1}{2\pi}\ln[r_i(x)] \quad in \quad 2D \\ w(x, x_i) &= \frac{1}{4\pi r_i(x)} \quad in \quad 3D \end{aligned} \tag{21}$$

Therefore, manipulation of the second residual R_w in Eqn. (18) leads to:

$$\int_\Omega \left[\sum_{j=1}^{N} \beta_j \psi_j(x) - \sum_{j=1}^{N} \alpha_j \phi_j(x)\right] w(x, x_i) d\Omega = 0 \tag{22}$$

After rearranging:

$$\sum_{j=1}^{N} \beta_j \int_\Omega \psi_j(x) w(x, x_i) d\Omega = \sum_{j=1}^{N} \alpha_j \int_\Omega \phi_j(x) w(x, x_i) d\Omega \tag{23}$$

Defining the weighted matrices $[\phi_w]$ and $[\psi_w]$ as:

$$[\phi_w] = \int_\Omega \phi_j(x) w(x, x_i) d\Omega \tag{24}$$

And:

$$[\psi_w] = \int_\Omega \psi_j(x) w(x, x_i) d\Omega \tag{25}$$

Allows expressing Eqn. (23) in matrix-vector form as:

$$[\psi_w]\{\beta\} = [\phi_w]\{\alpha\} \tag{26}$$

The weighted matrices $[\phi_w]$ and $[\psi_w]$ in Eqns. (24) and (25) can be obtained by standard numerical integration realizing that the weighting functions $w(x, x_i)$ as defined in Eqn. (21) are singular at the expansion points $x = x_i$. However, simple adaption of the numerical integration scheme will mitigate this issue as the singularity is weak.

Introducing the coefficients $\{\alpha\}$ from Eqn. (20) into Eqn. (26) and solving for the coefficients $\{\beta\}$ results in:

$$\{\beta\} = [\psi_w]^{-1}[\phi_w][\phi]^{-1}\{f\} \tag{27}$$

The coefficients $\{\beta\}$ in Eqn. (27) are the expansion coefficients for the function $f_w(x)$ in Eqn. (13). These are coefficients obtained through a weighted approach and therefore the resulting function $f_w(x)$ is not 'anchored' at the expansion points $x_i \therefore i = 1 \ldots N$, yielding smooth and accurate derivative fields. In addition, as it can be seen in Eqn. (27), this expansion also offers the advantage of being able to be performed without knowledge of the exact distribution of the function $f(x)$ but rather relies only on the scattered information $\{f\}$, achieving the two desired goals critical in the implementation of this expansion in a Localized Meshless Method for the solution of governing differential equations.

As it will be shown in the next section, the expansion coefficients α_j and β_j will not be explicitly computed. Instead, algebraic manipulations of the expansion formulae will allow expressing the derivative fields directly in terms of scattered values of the function within a localized influence region. Therefore, having two sets of expansion coefficients does not mean additional overhead in the solution process as these will be built implicitly into the approximation.

LOCALLY-INTEGRATED MESHLESS (LIM) METHOD

The hybrid RBF expansion presented in the previous section can be implemented in the formulation of a Locally-Integrated Meshless (LIM) method. Consider the topology of N influence points around the data center x_c seen in Figure 5.

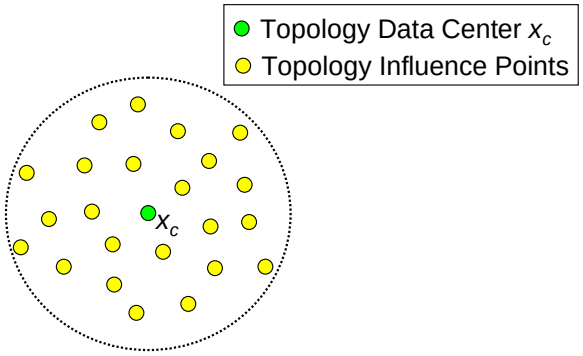

Figure 5 Illustration of a topology around a data center, x_c.

If any order derivative operator L of the function $f(x)$ is sought at the data center x_c within the influence domain Ω, $Lf(x_c)$, it can be approximated using the weighted expansion $f_w(x)$ as:

$$Lf(x_c) \approx Lf_w(x_c) = \sum_{j=1}^{N} \beta_j L\psi_j(x_c) \quad (28)$$

Introducing the expansion coefficients $\{\beta\}$ in Eqn. (27) and writing the expression in matrix-vector form results in:

$$\begin{aligned} Lf(x_c) &\approx \{L\psi_c\}^T \{\beta\} \\ &= \{L\psi_c\}^T [\psi_w]^{-1} [\phi_w][\phi]^{-1} \{f\} \end{aligned} \quad (29)$$

Where $\{L\psi_c\}$ is the vector of expansion function derivatives $L\psi_j(x_c)$ at the data center x_c. Furthermore, defining:

$$\{L\}^T = \{L\psi_c\}^T [\psi_w]^{-1} [\phi_w][\phi]^{-1} \quad (30)$$

This allows approximating any order derivative L of the function $f(x)$ at a point x_c within the domain Ω simply as:

$$Lf(x_c) \approx \{L\}^T \{f\} \quad (31)$$

Where the weighted derivative interpolation vector $\{L\}$ in Eqn. (30) is only a function of the RBFs $\phi_j(x)$ and $\psi_j(x)$, the weighting functions $w(x, x_i)$, and the point distribution $x_i \therefore i = 1 \ldots N$. This feature is key to the implementation of this expansion approach in a Localized Meshless Method as the solution process would yield scattered function information $\{f\}$ whose derivatives must be approximated to be evolved in time or iterated until convergence. Again, the weighted matrices $[\phi_w]$ and $[\psi_w]$ in Eqn. (30) can be obtained by standard numerical integration. The adaptive numerical integration scheme can be easily implemented within the regular domain constructed as the localized topology or influence region over each data center. Moreover, as these operators are only space-dependent, they may be pre-computed and stored at the setup stage of a solution process and later employed during the time-marching or iteration scheme; therefore not imposing additional overhead on the solution process.

Implementation of the LIM Method

For the purpose of illustrating the implementation of the LIM approach to the solution of heat transfer and fluid flow problems, the advection-diffusion of energy equation will be employed. Advection-diffusion of energy in a flow field $\vec{V}$ of an incompressible fluid with constant density ρ, specific heat c_p, thermal conductivity k, without heat generation or viscous dissipation is governed by:

$$\rho c_p \left(\frac{\partial T}{\partial t} + \vec{V} \cdot \nabla T \right) = k \nabla^2 T \quad (32)$$

In order to arrive at a solution of Eqn. (32), the domain Ω, the boundary Γ, as well as a complete set of boundary conditions along with an initial condition for the temperature field T are required.

A time-marching scheme may be formulated to explicitly or implicitly march the solution from the initial condition. For instance, if a first-order explicit time-marching scheme is adopted for a 2D problem, the following form is arrived at:

$$T_i^{n+1} = T_i^n + \Delta t \left(\frac{k}{\rho c_p} \nabla^2 T - u \frac{\partial T}{\partial x} - v \frac{\partial T}{\partial y} \right)_i^n \quad (33)$$

Where u and v are the *x* and *y* components of the velocity field $\vec{V}$ respectively. In this case, the subscript i is an index for the location of the scattered data center within the domain while the superscripts n and $n+1$ indicate the previous and current time values separated by a time step Δt. Solutions of this equation using the LCM method and implementation of this time-marching scheme have been extensively shown by the authors in a variety of settings, see [41]-[51]. The current work concentrates on the approximation of the derivative fields present in Eqn. (33), $\nabla^2 T$, $\partial T / \partial x$, and $\partial T / \partial y$, using the LIM approach. That is, these derivative fields will be tested in extreme circumstances to show that the LIM method provides a robust alternative capable of accurately approximating these derivatives and hence allowing for a stable and accurate time-marching scheme implementation.

In order to arrive at a robust, accurate, and stable time-marching solution scheme, it is imperative to be able to accurately approximate the values of the derivative fields $\nabla^2 T$, $\partial T / \partial x$, and $\partial T / \partial y$ at any data center x_i using just scattered information from neighboring data centers. This can be accomplished by using the derivative interpolation vectors $\{L\}$ in Eqn. (30). In addition, the fact that these vectors depend only upon the location of the data centers x_c, the choice of RBFs $\phi_j(x)$ and $\psi_j(x)$, and the weighting functions $w(x, x_i)$, allows for the computation of these vectors to be performed at a pre-processing stage of the problem to later be used during the time-marching scheme, rendering the formulation very efficient.

The availability of such interpolation vectors $\{L\}$ derived using a weighted-residual approach rather than a collocation approach is essential for the stability of the solution scheme. Derivatives yielded through collocation can exhibit small perturbations due to the anchoring of the values at the data center. This behavior is propagated through the time-marching scheme and affects the stability of it. Derivative values yielded through a weighted-residual formulation offer an inherent smoothing behavior capable of mitigating these issues. In

addition, if the advection-diffusion problem is dominated by the convective derivatives $u\partial T/\partial x$ and $v\partial T/\partial y$, upwinding schemes can be easily implemented by evaluating the derivatives upstream of the data center using the same formulation presented in the previous section.

Derivative Field Approximation Test Case

To illustrate the accuracy in the approximation of the derivative fields a simple test case is presented by introducing a test function $T(x,y)$ as:

$$T(x,y) = e^{x+y}\left(x^2y^2 - 1\right)\sin\left(\frac{x}{3} + \frac{y}{2}\right) \qquad (34)$$

The function in Eqn. (34) does not represent a solution to the advection-diffusion equation (32) but rather an arbitrary function that exhibits extremes and non-monotonic behavior within the influence region to be selected. This will serve the purpose of validating the claims of accuracy of the derivative fields. A localized region of influence or topology for integration of the weighted-residual formulation was selected as a circle of radius $R = 1$ around the origin $(0,0)$. A total of $N = 13$ points were scattered in the topology. The choice of the test function in Eqn. (34) was made to ensure that its variability was high enough so that the function could exhibit highly non-linear and non-monotonic behavior within the region of influence as shown in Figure 6 along with the point distribution in the topology.

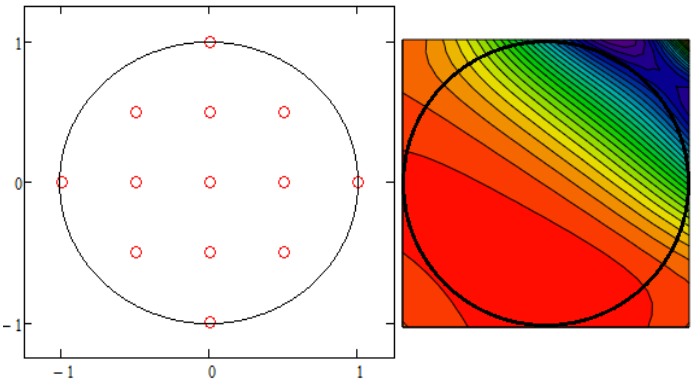

Figure 6 Point distribution and contour plot on region of interest

A comparison between the derivative values rendered by the Localized Collocation Meshless (LCM) approach and the Locally-Integrated Meshless (LIM) approach are presented in Table 2. These solutions reveal that the evaluation of the derivatives at the topology data center x_c by the LIM approach are more accurate in reference to the exact solution than those rendered by the LCM approach when applied to this highly non-linear and non-monotonic temperature distribution.

Table 2 Derivative values from LCM and LIM compared to exact solution

	Exact	LCM	LIM
$\partial T/\partial x$	-0.333	-0.305	-0.334
$\partial T/\partial y$	-0.500	-0.460	-0.486
$\nabla^2 T$	-1.667	-1.578	-1.726

LIM Method Example

The LIM method is now tested by approximating the solution of an advection-diffusion problem in a $10\times 1cm$ channel with laminar fully-developed flow with a developing thermal field. The fluid is air with density $\rho = 1.225kg/m^3$, specific heat $c = 1006.43J/kgK$, thermal conductivity $k = 0.0242W/mK$, and absolute viscosity $\mu = 1.79\cdot 10^{-5} kg/m\cdot s$. The velocity profile is parabolic with a maximum velocity at the horizontal center line $U = 0.25m/s$. The flow is incoming from the left with a bulk temperature $T_{in} = 273K$ while the channel top and bottom walls are kept at a temperature $T = 373K$. The outlet condition on the right-hand side is considered adiabatic. The meshless model is setup using 110 points distributed around the boundary and 250 collocation points uniformly distributed in the interior as seen in Figure 7. The LIM method approximation is compared to a solution provided by ANSYS Fluent using a finite volume mesh with 4825 nodes. The temperature contour plot shown in Figure 8 reveals excellent qualitative agreement between the Fluent and LIM approximations while Figure 9 shows very good quantitative agreement between these two approximations at 1/4, 1/2, 3/4, and the full length of the channel.

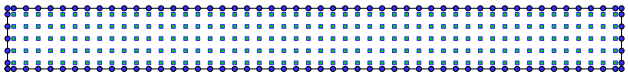

Figure 7 Meshless point distribution for advection-diffusion example in a channel.

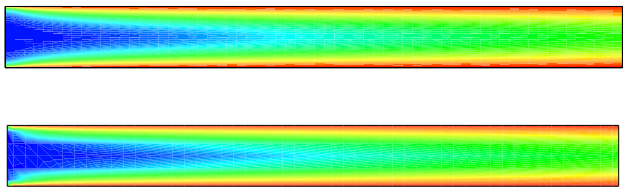

Figure 8 Fluent and LIM method temperature contour plots.

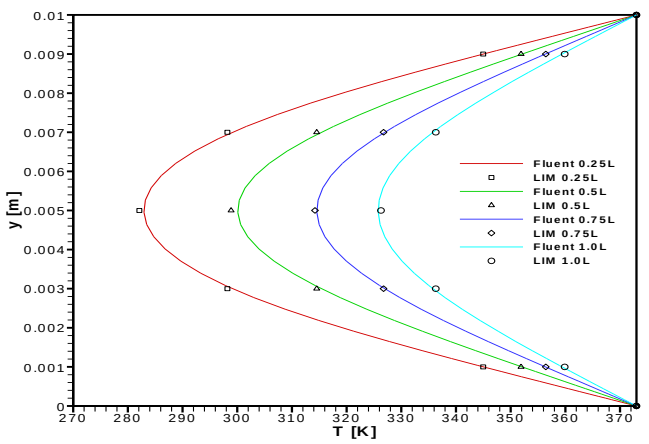

Figure 9 Fluent and LIM Temperature profiles at 1/4, 1/2, 3/4, and full length of the channel flow.

CONCLUSION

A new numerical solution scheme coined as the LIM (Locally-Integrated Meshless) method is formulated in this paper. As a Meshless formulation the LIM Method relies uniquely on a scattered non-ordered data point distribution within the domain of interest and does not require connectivity or polygonalization. In the LIM method formulation the field variable is approximated within localized overlapping regions containing a predetermined number of data points, as a linear combination of predefined expansion functions. These expansion functions are chosen in this study to be the well-known Hardy Multiquadrics Radial-basis functions (RBF) with center at the data points within each localized region. A weighted-residual integration is applied on each region to minimize the difference between the approximated field and the exact one. In order to circumvent the integration of an unavailable exact field, the residual integral is decomposed into a collocation integral and a fully-weighted integral, resulting in a formulation where the coefficients of the expansion can be expressed directly in terms of the values of the field variable at the data points. This approach allows mitigating the issues that arise when performing direct collocation where the resulting derivative fields are sensitive and inaccurate due to the 'anchoring' of the expansion to the data points. In contrast, the LIM method yields derivative fields that are smooth and accurate as they are rendered from a 'non-anchored' expansion while providing the ability to express the expansion coefficients, and thus the derivative fields, directly in terms of the scattered data within each local region. This combination of features is critical for the implementation of the LIM method as a robust, stable, and accurate solution scheme of governing differential equations. The LIM method is formulated for energy advection-diffusion problems, validated using a test function, and tested in a channel flow example yielding significantly accurate results.

REFERENCES

[1] Belytscho, T., Lu, Y.Y., and Gu, L., "Element-free Galerkin methods, *Int. J. Num. Methods*," Vol. 37, 1994, pp. 229-256.

[2] Atluri, S.N. and Shen, S., *The Meshless Method*, Tech. Science Press, Forsyth, 2002.

[3] Atluri, S.N. and Zhu, T., "A new meshless local Petrov-Galerkin (MLPG) approach in computational mechanics," *Computational Mechanics*, Vol. 22, 1998, pp. 117-127.

[4] Onate, E., Idehlson, S., Zienkiewicz, O.C., Taylor, R.L., and Sacco, C.,"A stabilized finite point method for analysis of fluid mechanics problems," Computer Methods in Applied Mechanics and Engineering, Vol. 139, 1996, pp. 315-346

[5] Liu, G.R., *Mesh Free Methods: Moving Beyond the Finite Element Method.*, CRC Press, Boca Raton, 2002.

[6] Melenk, J.M. and Babuska, I., "The partition of unity finite element method: basic theory and application," *Comp. Meth. Appl. Mechanics and Eng.*, Vol. 139, 1996, pp. 289- 316.

[7] Gu, Y.T., and Liu, G.R., "Meshless techniques for convection dominated problems," Computational Mechanics, Vol. 38, 2006, pp. 171–182.

[8] Gottlieb, D. and Orzag, S.A., *Numerical Analysis of Spectral Methods: theory and applications*, Society for Industrial and Applied Mathematics, Bristol, England, 1977.

[9] Maday, Y. and Quateroni, A., "Spectral and Pseudo-Spectral Approximations of the Navier-Stokes Equations," *SIAM J. Numerical Analysis*, 1982, Vol. 19, No. 4, pp. 761-780.

[10] Patera, A., "A Spectral Element Method of Fluid Dynamics: laminar flow in a channel expansion," *J. of Computational Physics*, 1984, Vol. 54, pp. 468-488.

[11] Macaraeg, M. and Street, C.L., "Improvement in Spectral Collocation Discretization Through a Multiple Domain Technique," *Applied Numerical Mathematics*, 1986, Vol. 2, pp. 95-108.

[12] Hwar, C.K., Hirsch, R., Taylor, T., and Rosenberg, A.P., "A Pseudo-Spectral Matrix Element Method for Solution of Three Dimensional Incompressible Flows and its Parallel Implementation," *J. of Computational Physics*, 1989, Vol. 83, pp. 260-291.

[13] Fasshauer, G, "RBF Collocation Methods as Pseudo-Spectral Methods," *Boundary Elements XVII*, Kassab, A., Brebbia, C.A. and Divo, E. (eds.), WIT Press, 2005, pp. 47-57.

[14] Powell, M.J.D., "The Theory of Radial Basis Function Approximation," in *Advances in Numerical Analysis, Vol. II*, Light, W., ed., Oxford Science Publications, Oxford, 1992. pp. 143-167.

[15] Buhmann, M.D., Cambridge *Radial Basis Functions: Theory and Implementation* University Press, Cambridge, 2003.

[16] Dyn, N., Levin, D., and Rippa, S., "Numerical Procedures for Surface Fitting of Scattered Data by Radial Basis Functions," *SIAM J. of Sci. Stat. Computing*, 1986, Vol. 7, No. 2, pp. 639-659.

[17] Hardy, R.L., Multiquadric Equations of Topography and Other Irregular Surfaces, *Journal of Geophysical Research*, Vol. 176, pp. 1905-1915.

[18] Kansa, E.J., "Multiquadrics- a scattered data approximation scheme with applications to computational fluid dynamics I-surface approximations and partial derivative estimates," *Comp. Math. Appl.*, Vol. 19, 1990, pp. 127-145.

[19] Kansa, E.J., "Multiquadrics- a scattered data approximation scheme with applications to computational fluid dynamics II-solutions to parabolic, hyperbolic and elliptic partial differential equations," *Comp. Math. Appl.*, Vol. 19, 1990, pp. 147-161.

[20] Kansa, E.J. and Hon, Y.C., "Circumventing the Ill-Conditioning Problem with Multiquadric Radial Basis Functions: Applications to Elliptic Partial Differential Equations," *Comp. Math. Appl.*, 2000, Vol. 39, pp. 123-137.

[21] Franke, R., "Scattered data interpolation: Test of some methods," *Math. Comput.*, Vol. 38, 1982, pp. 181-200.

[22] Mai-Duy, N. and Tran-Cong, T., "Mesh-Free Radial Basis Function Network Methods with Domain Decomposition for Approximation of Functions and Numerical Solution of Poisson's

Equation," *Engineering Analysis with Boundary Elements*, 2002, Vol. 26, pp. 133-156.
[23] Cheng, A.H.-D., Golberg, M.A., Kansa, E.J., Zammito, G., "Exponential Convergence and H-c Multiquadric Collocation Method for Partial Differential Equations," *Numerical Methods in P.D.E.*, Vol. 19, No. 5, 2003, pp. 571-594.
[24] Divo, E. and Kassab, A.J., Boundary Element Method for Heat Conduction: with Applications in Non-Homogeneous Media, Topics in Engineering Series Vol. 44, WIT Press, Billerica, MA, 2002.
[25] Kassab, A.J., Wrobel, L.C., Bialecki, R.A., and Divo, E., "Boundary Elements in Heat Transfer," Chapter 4 in Handbook of Numerical Heat Transfer, Minkowycz, W. and Sparrow, E.M. (eds.), John Wiley and Sons, New York, NY, John Wiley and Sons, Vol. 1, 2nd Edition, pp. 125-166, 2005.
[26] Sarler, B. and Vertnik, R., "Local Explicit Radial Basis Function Collocation Method for Diffusion Problems," *Computers and Mathematics with Applications*,Vol. 51, No. 8, 2006, pp. 1269-1282.
[27] Vertnik, R. and Sarler, B.,"Meshless local radial basis function collocation method for convective-diffusive solid-liquid phase change problems," *International Journal of Numerical Methods for Heat and Fluid Flow*, Vol. 16, No. 5, 2006, pp. 617-640.
[28] Vertnik, R., Zaloznik, M. and Sarler, B., "Solution of transient direct-chill aluminium billet casting problem with simultaneous material and interphase moving boundaries by a meshless method," *Engineering Analysis with Boundary Elements*, Vol. 30, No. 10, 2006, pp. 847-855.
[29] Divo, E., Kassab, A.J., and Erhart, K., "Parallel Domain Decomposition BEM Techniques for Steady and Transient Heat Transfer", Chapter 5 in Parallel BEM and Mesh Reduction Methods, Popov, V., Power, H., and Skerget, L. (eds.), WIT Press, Billerica, MA, pp. 147-186, 2007.
[30] Divo, E.A., Kassab, A.J. and Rodriguez, F., "Parallel Domain Decomposition Approach for large-scale 3D Boundary Element Models in Linear and Non-Linear Heat Conduction," *Numerical Heat Transfer, Part B, Fundamentals*, Vol. 44, No. 5, 2003, pp. 417- 437.
[31] Erhart, K., Divo, E., and Kassab, A.J., "A Parallel Domain Decomposition Boundary Element Method Technique for Large-Scale Transient Heat Conduction Problems," Engineering Analysis with Boundary Elements, Vol. 30, No. 7, pp. 553-563, 2006.
[32] Gamez, B., Ojeda, D., Divo, E., Kassab, A., and Cerrolaza, M., "Parallelized Iterative Domain Decomposition Boundary Element Method for Thermoelasticity," Engineering Analysis with Boundary Elements, Vol. 32, pp. 1061-1073, 2008.
[33] Divo, E., Kassab, A.J., Mitteff, E., and Quintana, L. "A Parallel Domain Decomposition Technique for Meshless Methods Applications to Large-Scale Heat Transfer Problems," *ASME Paper: HTFED2004-56004*.
[34] Divo, E. and Kassab, A.J., "Effective Domain Decomposition Meshless Formulation of Fully-Viscous Incompressible Fluid Flows," *Boundary Elements XVII*, Kassab, A., Brebbia, C.A. and Divo, E. (eds.), WIT Press, 2005, pp. 67-77.
[35] Divo, E. and Kassab, A.J., "A Meshless Method for Conjugate Heat Transfer," *Proceedings of ECCOMAS Coupled Problems 2005*, M. Papadrakis, E. Oñate and B. Schrefler (Eds.), Santorini, Greece, 2005.
[36] Divo, E. and Kassab, A.J., "A Meshless Method for Conjugate Heat Transfer Problems," *Engineering Analysis*, Vol. 29, No. 2 , 2005, pp. 136-149.
[37] Gerace, S.A., Divo, E., and Kassab, A.J., "A Localized Radial-Basis-Function Meshless Method Approach to Axisymmetric Thermo-Elasticity," *AIAA Paper 2006-3788*.
[38] Divo, E. and Kassab, A.J., "Modeling of Convective and Conjugate Heat Transfer by a Third Order Localized RBF Meshless Collocation Method," *Proc. of NHT-05 Eurotherm82*, Bialecki, R.A. and Nowak, A.J. (eds.), 2005, pp. 357-366.
[39] Divo, E., Kassab, A.J., and El Zahab, Z., "Parallel Domain Decomposition Meshless Modeling of Dilute Convection-Diffusion of Species," *Proceedings of BEM27/MRM*, Kassab, A.J., Brebbia. C.A. and Divo, E.A. (eds.), Computational Mechanics Publications, Southampton, U.K.,2005, pp. 79-90.
[40] Divo, E. and Kassab, A.J., "Iterative Domain Decomposition Meshless Method Modeling of Incompressible Flows and Conjugate Heat Transfer," *Engineering Analysis*, Vol. 30, No. 6, 2006, pp. 465-478.
[41] Divo, E. and Kassab, A.J., "An Efficient Localized RBF Meshless Method for Fluid Flow and Conjugate Heat Transfer," *ASME Journal of Heat Transfer*, 2007, Vol. 129, pp. 124-136.
[42] Divo, E. and Kassab, A., "Localized Collocation Meshless Method (LCMM) for Convectively Dominated Flows," *Proceedings of the 8th World Congress on Computational Mechanics and 5th European Congress on Computational Methods in Applied Sciences and Engineering*, Venice, Italy, June 30 - July 5, 2008.
[43] Divo, E. and Kassab, A.J., "Localized Meshless Modeling of Natural Convective Viscous Flows," Numerical Heat Transfer, Part A: Fundamentals, Volume 53, Issue 6, June 2008, pages 487-509.
[44] Mitteff, E., Divo, E., and Kassab, A.J., "Automated Point Distribution and Parallel Segmentation for Meshless Methods," *Proceedings of CIMENICS 2006, 8th International Congress of Numerical Methods in Engineering and Applied Sciences.* held on Margarita Island, Venezuela, March 20-24, 2006, Gamez B., Ojeda D., Larrazabal G., and Cerrolaza M. (eds.), Sociedad Venezolana de Methodos Numericos en Ingenieria, Valencia, Venezuela, pp. 93-100.
[45] El Zahab, Z., Divo, E., and Kassab, A.J., "A Localized Collocation Meshless Method (LCMM) for Incompressible Flows CFD Modeling with Applications to Transient Hemodynamics," Engineering Analysis with Boundary Elements, Vol. 33, No. 8-9, pp. 1045-1061, 2009.
[46] Divo, E., Kassab, A.J., Reddi, L., Kakuturu, S., and Hagen S., "RBF-FVM Numerical Solution of the Poro-Elasticity Levee Problem with Time-Varying Boundary Conditions," Proceedings of ECCOMAS Couple Problems 2009, Ischia Island, Italy, June 8-10, 2009.
[47] Gerace, S., Erhart, K., Divo, E., and Kassab, A.J., "Adaptively Refined Hybrid FDM-RBF Meshless Scheme with Applications to Laminar and Turbulent Viscous Fluid Flows," Computer Modeling in Engineering and Science, Vol. 81, No.1, pp.35-67, 2011.
[48] Gerace, S., Erhart, K., Kassab, A.J., and Divo, E., "A Model-Integrated Localized Collocation Meshless Method for Large Scale Three-Dimensional Heat Transfer Problems," Computer Assisted Methods in Engineering and Science, 20: 207–225, 2013.
[49] Kelly, J., Divo, E., and Kassab, A.J., "Numerical Solution of the Two-Phase Incompressible Navier-Stokes Equations Using a GPU-Accelerated Meshless Method," Engineering Analysis with Boundary Elements, 40: 36-49, 2014.
[50] Erhart, K. Kassab, A.J. and Divo, E., "An Inverse Localized Meshless Technique for the Determination of Non-Linear Heat Generation Rates in Living Tissues," *International Journal of Numerical Methods for Heat and Fluid Flow*, Vol. 18, No. 3/4, 2008, pp. 401-414.
[51] El Zahab, Z., Divo, E., and Kassab, A.J., "A Meshless CFD Approach for Evolutionary Shape Optimization of Bypass Grafts Anastomoses," Journal Inverse Problems in Science and Engineering, Vol. 17, No. 3, 411-435, 2009.